

Novel technique to measure the microwave response of high T_c superconductors between 4.2 and 200 K

S. Sridhar and W. L. Kennedy

Physics Department, Northeastern University, Boston, Massachusetts 02115

(Received 21 October 1987; accepted for publication 3 February 1988)

We have devised and implemented a novel technique that has the required sensitivity to enable measurements of the complex surface impedance (Z_s) of high T_c superconducting materials between 4.2 K and at least 200 K. The essential idea is to employ a superconducting high- Q cavity resonator operated at an ambient temperature of 4.2 K. The sample, mounted on a sapphire rod, is placed inside the cavity at a high magnetic field location, and is thermally insulated from the cavity walls, enabling external control of the sample temperature between 4.2 and 200 K. The cavity characteristics are dominated by the sample properties—the Pb walls maintained at 4.2 K contribute negligibly. Measurement of the cavity Q and resonant frequency enables the measurement of Z_s as a function of the sample temperature. The technique is applicable to both bulk and thin-film materials. We have used this technique with success to measure Z_s at 9.58 GHz, for bulk $Y_1Ba_2Cu_3O_y$ and $La_{1.85}Sr_{0.15}CuO_4$ over a temperature range from 4.2 to 100 K.

INTRODUCTION

The recent discovery¹ of the high T_c oxide superconductors, while opening up a wealth of exciting possibilities, also poses new challenges for experimental techniques specifically designed to study these superconductors. We have been involved^{2,3} in rf and microwave studies of the 40- and 93-K families of superconductors with two broad objectives: first, to study the nature of the superconducting state, and second, to evaluate the potential of these materials for applications at frequencies from 1 MHz to 100 GHz. Such studies are of particular importance because electromagnetic probes are sensitive only to the electronic state while other traditional probes (specific heat, ultrasonic attenuation) are strongly influenced by the phonon system, which is heavily populated at the high temperatures involved with these materials.

The parameters that need to be measured are the surface resistance R_s , and the surface reactance X_s (complex surface impedance $Z_s = R_s + iX_s$), preferably over a broad range of temperature and frequency. These quantities vary strongly upon cooling through the transition temperature T_c . R_s , in particular, can vary over four orders of magnitude between T_c and $0.3T_c$ for a superconducting material to which the BCS theory of superconductors is applicable.

Since the absorption in a superconductor is very low,⁴ special techniques are required to study the microwave response of superconductors. A useful method of achieving the required sensitivities is to employ⁵ very high Q (10^4 – 10^{12}) cavities. For materials such as Pb ($T_c = 71$ K), Nb (9 K), and NbN (18 K) it is possible to fabricate the entire cavity using the material, this gives the greatest sensitivity achievable, limited by the properties of the superconducting material only. For materials with very low T_c 's, one can use a cavity made of a higher T_c material, e.g., measurements⁶ on Sn ($T_c = 3.8$ K) using Pb-plated cavities. An entirely different

method⁷ is to directly measure the microwave absorption in the superconductor by calorimetric means. This method has been applied to the study of A-15 superconducting films. None of the above methods, however, can be used to study high T_c (> 20 K) superconductors over a broad temperature range. The absorption calorimetric technique, which requires measuring very small temperature changes, is quite insensitive at the high temperatures involved (above 20 K).

We had earlier managed^{2,3} to study $Y_1Ba_2Cu_3O_y$ and $La_{1.85}Sr_{0.15}CuO_4$ using a Cu TE₀₁₁ cavity operating at 9.58 GHz, where the bottom wall was made of the high T_c superconducting material. Useful results were only obtained between $0.8T_c$ and T_c . At lower temperatures, the R_s of the sample was too low to be measurable in the presence of the Cu absorption background. Attempts are currently underway to fabricate cavities made of the materials. While the background problem would be eliminated, the fabrication of the cavity is not trivial.

To overcome these limitations we have devised a novel technique that has the required sensitivity to enable measurements of R_s between 4.2 and at least 200 K. The essential idea is to employ a Pb-plated Cu high- Q cavity operated at an ambient temperature of 4.2 K. The sample, mounted on a sapphire rod, is placed inside the cavity at a high B-field location (center of cavity), and is thermally insulated from the cavity walls, enabling variability of sample temperature. Measurement of the cavity Q and resonant frequency, which are dominated by the sample properties, enables the measurement of R_s and X_s as a function of sample temperature. The technique is applicable to bulk samples as well as thin films deposited on appropriate substrates.⁸

We have used this technique with success to measure R_s and X_s at 9.58 GHz for $Y_1Ba_2Cu_3O_y$ and $La_{1.85}Sr_{0.15}CuO_{4-\delta}$ over a temperature range from 4.2 to 100 K.

I. DESCRIPTION OF APPARATUS AND MEASUREMENT TECHNIQUE

A right cylindrical cavity (inner dimensions 4.127-cm diameter \times 4.107-cm long) was made using oxygen-free high conductivity (OFHC) Cu. It was fabricated in three pieces, and the pieces were electroplated with Pb following the technique of Ref. 9. The top plate has a central pumping hole (6.35-mm diameter), and two coupling holes (6.35-mm diameter) placed symmetrically at a distance 1.842 cm from the center. The bottom plate has one centrally located hole (0.381 cm diameter), through which the sample is inserted into the cavity. The three-piece cavity resonator was mounted in an alignment frame, supported on the top by a stainless-steel Dewar probe (10.16-cm diameter \times 1-m long) and, on the bottom, with a sealed Cu cup (10.16-cm diameter \times 10.16-cm long) with a removable bottom. Indium seals were used so that the entire assembly was vacuum tight. Superconducting operation of the cavity at 4.2 K was accomplished using a bath of liquid ^4He .

The sample (typically 3-mm-diameter \times 1-mm-thick disk) was mounted on a sapphire rod (3-mm diameter \times 52-mm long) using a tiny dot of vacuum grease. The sample and rod was inserted into the cavity, along its axis from the bottom, such that the sample is stationed 2.054 cm from the bottom wall. Support and adjustment of the rod was provided by a stainless-steel tube which was brazed to the removable Cu bottom plate (Fig. 1). Control of the sample temperature was accomplished using an external temperature controller, with a heating coil and Si diode thermometer attached to the sapphire rod outside the cavity.

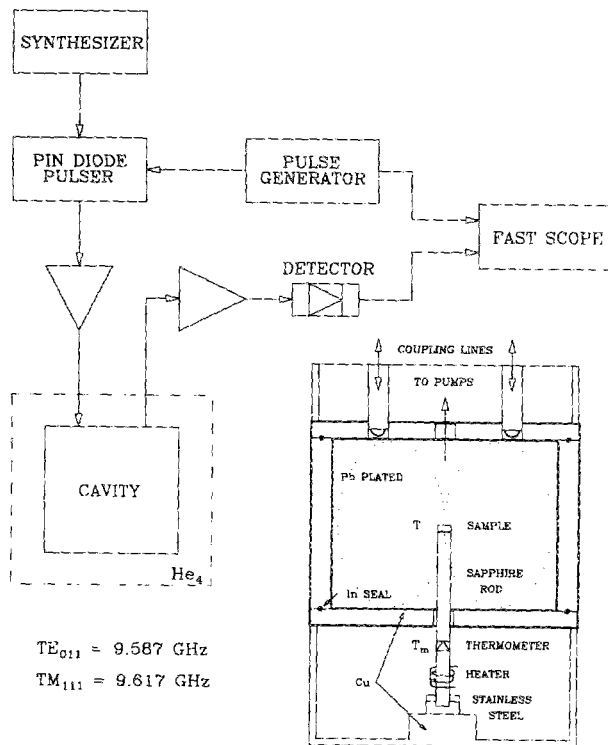


FIG. 1. Block diagram of the experimental apparatus. The inset shows the details of the cavity configuration.

Microwaves were coupled into and out of the resonator from the top, through two adjustable 50- Ω coaxial lines, each terminated in a loop. The magnetic field lines in the loop "look into" the resonator through small circular waveguide sections ending in symmetrically placed coupling holes (3.96-mm diameter) located at a low field region of the resonator.

We operate the cavity at very low rf fields ($\sim 10^{-3}$ G), where we do not observe a field dependence. Pulsed microwave power was fed into one port and the transmitted signal observed, after detection, on a fast scope (Fig. 1). The Q was determined using the decay method from the time constant τ , and $Q = \omega_0\tau$. The resonant frequency (f_0) was directly obtained from the synthesizer readout.

One very useful feature of this design is the ability to vary the coupling to the resonator by moving the lines in and out along the axis of the resonator. Thus it is possible⁶ to achieve critical coupling and weak coupling over a wide range of the resonator quality factor Q (10^4 – 10^{12} , in principle).

II. THERMAL ANALYSIS OF SAMPLE HEATING

It is important to assess the thermal characteristics of the sample mounting assembly. The important parameters that determine successful operation are: the temperature corrections due to spatial separation of the sample and sensing thermometer, the thermal time constant of the assembly, and the overall power consumption.

As indicated in Fig. 1, the point of temperature sensing and the localized heating are removed from the sample location, being outside the cavity along a length (l) on the sapphire rod. A simple estimate of the difference between the sample (T) and the measured (T_m) temperatures, taking into account the thermal conduction and radiation losses of the sapphire and sample, is given by

$$T_m - T \approx \frac{\sigma}{K_s} l \left(1 + \frac{2}{a} (l + t) \right) T_m^4, \quad (1)$$

where σ is the Stefan-Boltzmann constant, K_s the thermal conductivity of sapphire, a the radius of the rod, and t the thickness of the sample. In this estimate we have assumed a uniform thermal gradient along the rod, included the radiative losses in vacuum, and neglected the losses from the rod/sample interface and thermal gradient across the sample. The emissivity of all materials is taken to be unity. Note that for small l the σ/K sapphire ratio dominates the correction, such that even for temperatures as high as 200 K the correction is only of order mK, and $T \approx T_m$. Using $K_s \approx 60 \text{ W cm}^{-1} \text{ K}^{-1}$, $l = 2.6 \text{ cm}$, $a = 1.5 \text{ mm}$, and $t = 1 \text{ mm}$, we estimate a temperature correction of 0.85 mK, at 100 K. It is due entirely to the excellent thermal properties of sapphire that these temperature corrections are negligible.

The thermal time constant (τ_{thermal}) follows directly from considerations of energy conservation and power transfer, and is given by

$$\tau_{\text{thermal}} \approx m_s c_s l / \pi a^2 K_s, \quad (2)$$

where m_s is the mass and c_s the specific heat of sapphire. Using $m_s = 701.55 \text{ mg}$ and $c_s = 0.019 \text{ J/g K}$ we obtain

$\tau_{\text{thermal}} = 6.1$ ms, sufficiently small enough that it does not affect the measurements.

Referring to Fig. 1, we note the heating assembly has two conduction paths to the ${}^4\text{He}$ reservoir; that through radiation losses from the sample and rod to the resonator, and through the bottom stainless-steel mount. To limit the conduction paths, the entire cavity and sample mount is maintained in high vacuum, and the rod is mounted on a very thin (thickness t_{ss}) stainless-steel cylinder of length l_{ss} . In fact, this path dominates the power consumption (P) requirement of the apparatus, and is given by

$$P = \frac{\pi t_{\text{ss}}}{l_{\text{ss}}} (2R_{\text{ss}} - t_{\text{ss}}) K_{\text{ss}} (T_m - 4.2), \quad (3)$$

where K_{ss} is the thermal conductivity and R_{ss} is the outside diameter of the stainless-steel cylinder. Using $K_{\text{ss}} \approx 0.1$ W cm $^{-1}$ K $^{-1}$, $l_{\text{ss}} = 26$ mm, $t_{\text{ss}} = 0.2$ mm, and $R_{\text{ss}} = 6.35$ mm, we estimate $P = 108$ mW for $T_m = 40$ K and $P = 289$ mW for $T_m = 100$ K. The required power levels are easily obtained using the temperature controller. The sample microwave absorption is directly estimated to be less than $1 \mu\text{W}$ (corresponding to an axial magnetic field of < 10 mG), and is further pulsed with a duty cycle of 100. Thus the direct microwave heating does not affect stable operation. In application we find that temperature control is remarkably stable and precise (to within 0.05 below 20 K, and 0.2 above) with only modest ${}^4\text{He}$ boil off, using a standard temperature controller (DRC-82C).¹⁰

III. ELECTRODYNAMIC BASIS OF THE MEASUREMENT

All measurements were done using the TE_{011} mode of the resonator.¹¹ This mode was chosen as it has no electric fields at the cavity surface thus minimizing spurious absorption due to possible dielectric surface layers. Further there are no currents traversing the In joints connecting the three cavity pieces. We note, however, that the field perturbations due to the central pumping and sample insertion holes, on the top and bottom of the cavity, lift the degeneracy between the TE_{011} and TM_{111} modes. As well, the lack of azimuthal symmetry due to the coupling holes, further lifts the degeneracy of the TM_{111} mode into TM_{111}^{\pm} modes.

The TE_{011} configuration is well suited as a probe of the microwave response of a small, axially and centrally located sample. In this region we expect uniform axial magnetic field (Fig. 1). In these measurements any effects of the transverse electric fields, field perturbations and mode mixing, were determined by numerical computation to be negligible for small samples.

The quality factor Q of the cavity operating in a specified mode is given by the ratio of the energy stored to that absorbed by the cavity and sample¹²

$$Q = \mu_0 \omega_0 \frac{\int (B^2 + E^2) dV_{\text{cavity}}}{R_{s,\text{Pb}} \int B^2 dA_{\text{Pb}} + R_s \int B^2 dA_s} = \frac{\omega U_0}{\alpha R_{\text{Pb}} + \beta R_s}, \quad (4)$$

where $R_{s,\text{Pb}}$ and R_s are the surface resistances of the Pb walls

and the sample, respectively, and U_0 is the stored energy density in the cavity. A_{Pb} and A_s refer to the surface areas of the Pb and the sample, respectively, and α and β are geometric factors associated with the cavity mode and the sample geometry. The surface resistance of the sample can be expressed in terms of the measured Q 's as

$$R_s = \gamma_s \left(\frac{1}{Q(T)} - \frac{1}{Q_{\text{Pb}}} \right), \quad (5)$$

where $Q_{\text{Pb}} (= \omega U_0 / \alpha R_{s,\text{Pb}})$ is the measured Q without the sample, γ_s is a geometric factor given by $\omega_0 U_0 / \beta$. As indicated by Fig. 2, Q_{Pb} is not a severely limiting factor for a superconductivity cavity, allowing a broad range of measurement.

Changes in the surface reactance (X_s) are measurable as shifts in the resonant frequency of the cavity. The relationship between the frequency shift and the penetration depth (which is proportional to the reactance) is given by

$$\delta f \equiv f_0 \frac{\int B^2 dV_s}{\int B^2 dV_{\text{Pb}}} = \frac{at}{2t+a} \frac{\Delta f}{\Delta \lambda},$$

or equivalently,

$$\begin{aligned} \Delta \lambda(T, T') &\equiv \lambda(T) - \lambda(T') \\ &= [at / \delta f(2t+a)] [f(T') - f(T)] \\ &\equiv \xi_s \Delta f(T), \end{aligned} \quad (6)$$

where T and T' refer to two different temperatures, t the sample thickness, and a the sample thickness.

A. Normalized R_s and λ_g

It is possible to determine with greater accuracy ($\sim 2\%$), the normalized surface resistance ratio $r \equiv R_s / R_n$, where $R_n \equiv R_s(T_c)$ ($T_c \equiv$ transition temperature). From Eq. (5)

$$r \equiv \frac{R_s}{R_n} = \frac{1/Q(T) - 1/Q_{\text{Pb}}(T)}{1/Q(T_c) - 1/Q_{\text{Pb}}(T_c)}. \quad (7)$$

Note that the geometric factor γ_s is eliminated.

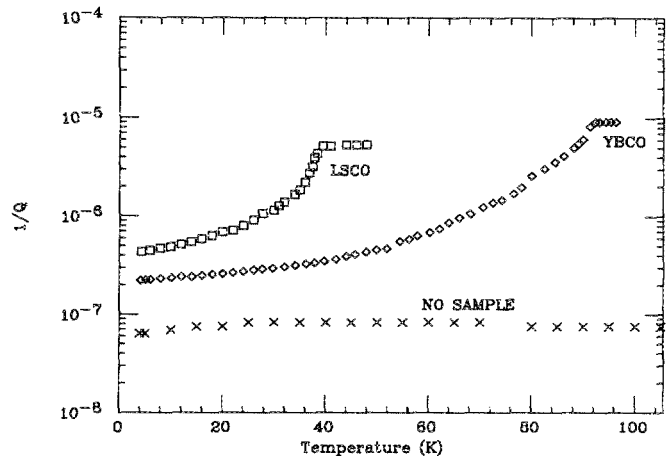


FIG. 2. $1/Q$ vs temperature for YBCO and LSCO samples, and with no sample.

Similarly it is also possible to eliminate ζ_s in the determination of $\Delta\lambda$, as follows:

$$\frac{\Delta\lambda(T)}{\Delta\lambda(T_c)} = \frac{\lambda(T) - \lambda(0)}{\lambda(T_c) - \lambda(0)} = \frac{f(0) - f(T)}{f(0) - f(T_c)}, \quad (8)$$

where $\lambda_n \equiv \lambda(T_c)$.

$$\gamma_s = \mu_0 \omega_0 \frac{L(R/X'_{01})^2 \{[(\omega_0/c)^2 + (\pi/L)^2] (R/X'_{01})^2 I_1 + I_0\}}{2a[a + (\pi R/X'_{01} L)^2 J_1^2 (X'_{01} a/R) I_+ + J_0^2 (X'_{01} a/R) I_-]} \quad (9)$$

We have assumed that the field at the two faces of the cylinder is uniform and equal to the unperturbed value at the sample center, and that the field at the side is equal to the unperturbed value at the location. In Eq. (9), J_p is the Bessel function of order p , X'_{01} the first zero of J_0 , c the velocity of light, L the cavity length, and R the cavity radius. The integrals I_p ($p = 0, 1$) and I_{\pm} are given by

$$I_p = \int_0^{X'_{01}} x J_p^2(x) dx$$

and

$$I_{\pm} \approx \frac{t}{2} \pm \frac{L}{4\pi} \sin\left[\pi\left(\frac{1+2t}{L}\right)\right].$$

Similarly,

$$\zeta_s = \frac{at}{2t+a} \times \frac{(\pi R/X'_{01} L)^2 I_1 + I_0}{2f_0[(\pi R/X'_{01} L)^2 I_1' I_+ + I_0' I_-]}, \quad (10)$$

where

$$I_p' = \int_0^{X'_{01}(a/R)} x J_p^2(x) dx, \quad p = 0, 1.$$

Numerical computations of γ_s and ζ_s were carried out for the samples used in this work. Given the assumptions, we expect γ_s and ζ_s to be accurate to a factor less than 2. For the small samples described, the estimates are actually better (Sec. IV).

It is important in a real measurement to minimize mixing of the TE₀₁₁ and the TM₁₁₁ modes due to introduction of the sample. Such mixing can occur if the entire configuration (cavity + sample) is not cylindrically symmetric, and would lead to spurious absorption since the TM modes have substantially lower Q . In the actual experiment, we have taken care to maintain the cylindrical symmetry, and to ensure that repeated insertion of the sample yields reproducible results. One method⁶ to check the effects of possible mode mixing is to cool the cavity through the In transition at 3.41 K—if substantial mixing is present, then the cavity Q should show a dramatic change since the TM₁₁₁ component is sensitive to the currents in the In O-ring.

IV. RESULTS

Figure 2 displays the raw data; in the form of $1/Q$ vs T , where T is the sample temperature. Data for the TE₀₁₁ mode

B. Absolute magnitudes of R_s and $\Delta\lambda$

Determination of the absolute magnitude of R_s and $\Delta\lambda$ requires computation of the geometric factors γ_s and ζ_s . For this however, some simplifying assumptions are required.

Using the mode equations¹² for the fields in the TE₀₁₁ mode, and a cylindrical sample of radius a and thickness t , we obtain the geometric factor

without a sample (but with the sapphire rod), and with YBCO ($T_c = 93$ K) and LSCO (39.5 K) are shown. It is apparent that over the entire sample temperature range, the sample absorption dominates and the background absorption due to the Pb cavity maintained at 4.2 K is negligible.

From the raw data one can determine surface resistance R_s using Eq. (5). R_s is displayed as a function of temperature in Fig. 3. The relative errors for R_s are less than 5%, and is the same (because $Q \ll Q_{Pb}$) over the entire temperature range.

The determination of the absolute magnitude of R_s was carried out as discussed in Sec. III. Using Eq. (5), and sample dimensions 2.7×0.6 mm for YBCO and 2.8×0.7 mm for LSCO, we estimate $\gamma_s = 4.82 \times 10^4$ Ω/sq and $R_n = 0.44$ Ω/sq for YBCO, and $\gamma_s = 4.32 \times 10^4$ Ω/sq and $R_n = 0.23$ Ω/sq for LSCO. These estimates are to be regarded as uncertain to a factor of 2, due to the uncertainties in the approximations of the analysis. It is also possible to estimate R_n from the normal state resistivity (ρ_n) using, $R_n = \sqrt{\pi f_0 \mu_0 \rho_n}$. This yields $R_n = 0.70$ Ω/sq for YBCO and 0.54 Ω/sq for LSCO, in good agreement with the direct measurements.

Figure 3 demonstrates quantitatively the microwave absorption characteristics of the high T_c superconductors. When the superconductor is cooled below T_c , electrons condense¹³ into pairs. This dramatically reduces the absorption in two ways—the pairs are effective in shielding the applied

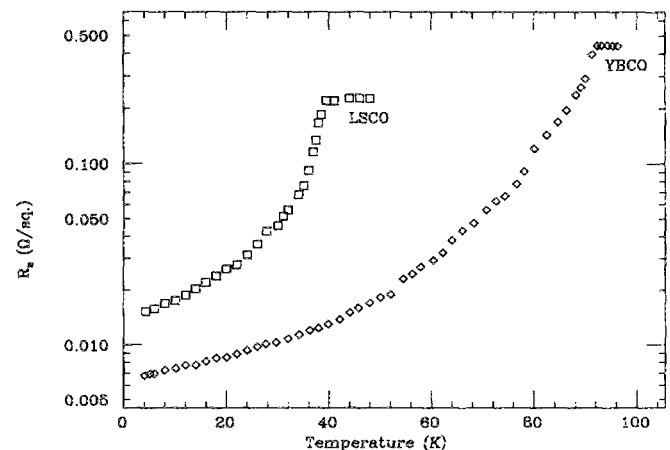


FIG. 3. Surface resistance R_s vs temperature T for YBCO and LSCO, determined from the raw data of Fig. 2.

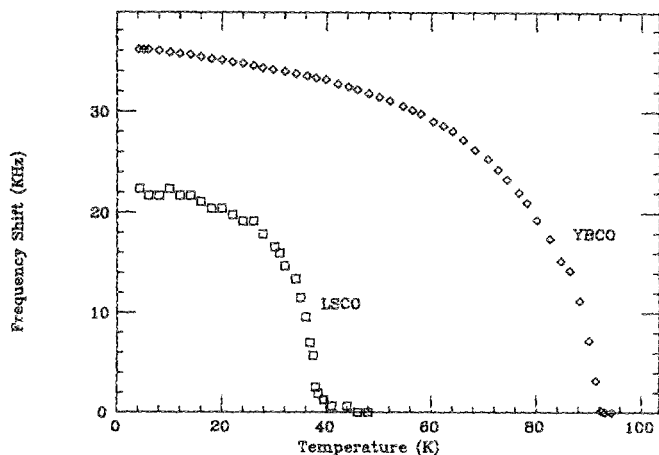


FIG. 4. Frequency shift Δf vs temperature T for YBCO and LSCO.

fields leading to reduced penetration, and also only the unpaired electrons (which are greatly reduced in number) contribute to the absorption. At low temperatures, $R_s \propto \exp(-\Delta/kT)$ according to the BSC s -wave theory, where Δ is the superconducting gap. It was to search for this behavior that we devised this experiment—the data of Fig. 3 do not apparently display an activated behavior. This may be due to a large residual absorption, or may be a fundamental effect. In any case, the data can be compared¹³ to detailed theories of the superconducting state.

The experiment also yields the shift in resonant frequency Δf of the cavity as a function of sample temperature, and this is displayed in Fig. 4. Δf is related to $\Delta\lambda$, the change in penetration depth of the sample, as discussed in Sec. III. The change in the penetration depth is plotted in Fig. 5 as the quantity $\Delta\lambda(T)$, where $\Delta\lambda(T) = \lambda(T) - \lambda(0)$. The penetration depth data can be understood as follows. The electron pairing below T_c improves the shielding and the relevant penetration depth λ decreases with temperature. The complete temperature dependence of λ is contained in Fig. 4.

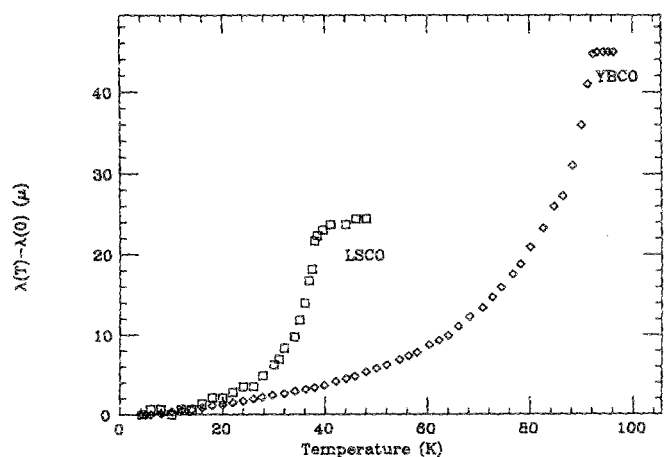


FIG. 5. Change in penetration depth $\lambda(T) - \lambda(0)$ vs temperature T for YBCO and LSCO, determined from data as in Fig. 4.

The total change in λ , viz. $\Delta\lambda(T_c)$ can be determined from the data using Eq. (6), for which determination of the geometric factor ζ_s is required [see Eq. (10)]. An estimate for ζ_s is given as $\zeta_s = 1.25 \text{ nm s}$ for the YBCO, and $\zeta_s = 1.09 \text{ nm s}$ for the LSCO samples, yielding $\Delta\lambda(T_c) = 44.39 \mu\text{m}$ for YBCO and $24.44 \mu\text{m}$ for LSCO. Unfortunately it is extremely difficult to measure $\lambda(0)$ absolutely, rather only changes $\Delta\lambda$ are determined. This drawback however, is common to all such measurements—it is generally difficult to measure λ absolutely without further assumptions.

Considerable information can be learned from data for R_s and λ such as is presented here. Temperature dependences of various parameters, such as the gap and density of states and the nature of the quasiparticle spectrum, can be inferred. Given a microscopic theory of superconductivity, e.g., BCS, a quantitative comparison to the data can also be made. We are currently pursuing such analyses, and details will be published elsewhere.¹⁴

V. DISCUSSION

The technique discussed above is quite successful in determining the microwave response of high T_c and other superconductors. Both R_s and λ are measurable over an extremely wide range of temperature, from 1.5 to 200 K and possibly higher. By maintaining the superconductivity cavity at a low temperature (here 4.2 K), good sensitivity is achievable. The sensitivity is determined by the cavity background Q , and a geometrical factor (equivalent to a filling factor) determined by sample dimensions. For an optimum cylindrical sample of dimensions 3.8 mm diameter \times 4.1 mm, the estimated lower measurable limit for $R_s = \gamma_s/Q_c$ is $4.6 \times 10^{-4} \Omega/\text{sq}$ and for $\Delta\lambda = \zeta_s$ is 0.05 nm (assuming a minimum frequency resolution of 1 Hz). A tenfold increase in R_s can be achieved by operating the Pb cavity at 1.5 K, enabling measurements of $R_s \approx 10^{-5} \Omega/\text{sq}$. Possibly higher sensitivities can be achieved with Nb or NbN cavities.

We have successfully demonstrated the technique by measurements on $\text{Y}_1\text{Ba}_2\text{Cu}_3\text{O}_7$ and $\text{La}_{1.85}\text{Sr}_{0.15}\text{CuO}_4$. Further experiments are underway exploring several factors: material preparation effects, single-crystal microwave response, frequency dependence, and magnetic field dependence.

ACKNOWLEDGMENTS

We thank H. Hamdeh for initial assistance, P. Taborek for useful discussions, and R. J. Ahlquist and S. DiCiaccio for technical assistance. This work was supported in part by Northeastern University Research funds, and by the Jet Propulsion Laboratory—NASA (No. NAS7-918/RE-210).

¹J. Bednorz and K. A. Müller, *Z. Phys. B* **64**, 189 (1986); M. K. Wu, J. R. Ashburn, C. J. Torng, P. H. Hor, R. L. Meng, L. Gao, Z. J. Huang, Y. Q. Wang, and C. W. Chu, *Phys. Rev. Lett.* **58**, 908 (1987); R. J. Cava, B. Batlogg, R. B. Van Dover, D. W. Murphy, S. Sunshine, T. Siegrist, J. P. Remick, E. A. Reitman, S. Zahurak, and G. P. Espinosa, *Phys. Rev. Lett.* **58**, 1676 (1987).

²S. Sridhar, H. Hamdeh, and H. Deng, *Phys. Rev. V*, Vol. 1 (1987).

³S. Sridhar, C. A. Shiffman, and H. Deng, *Phys. Rev. B* **36**, 2301 (1987).

⁴W. H. Hartwig and C. Passow, in *Applied Superconductivity*, edited by V.

L. Newhouse (Academic, New York, 1975), Vol. II.

⁵J. P. Turneaure, Ph.D. thesis, Stanford University, 1969 (unpublished).

⁶S. Sridhar, *J. Appl. Phys.* **62**, 159 (1988).

⁷L. H. Allen, M. R. Beasley, R. H. Hammond, and J. P. Turneaure, *IEEE Trans. Magn.* **MAG-23**, 1405 (1987).

⁸Other techniques and results have recently been reported in Proceedings of the Third Workshop on rf Superconductivity, edited by K. Shepard, Argonne, IL (unpublished).

⁹G. J. Dick, J. R. Delayen, and H. C. Yen, *Proc. IEEE Trans. Nucl. Sci.* **NS-24**, 1130 (1977).

¹⁰Manufactured by Lakeshore Cryotronics Inc., Westerville, OH 43081.

¹¹A. F. Harvey, *Microwave Engineering* (Academic, London, 1963).

¹²J. D. Jackson, *Classical Electrodynamics* (Wiley, New York, 1975).

¹³M. Tinkham, *Introduction to Superconductivity* (McGraw-Hill, New York, 1979).

¹⁴S. Sridhar and W. L. Kennedy (to be published).